Electronic Supplementary Information

In situ generated Pb nanoclusters on basic lead carbonate ultrathin nanoplates as an effective heterogeneous catalyst

Xiaoli Yu,[a] Qi Diao,[a] Xiaokai Zhang,*[b] Yong-Ill Lee,[c] Hong-Guo Liu*[a]

[a] *Key Laboratory for Colloid and Interface Chemistry of Education Ministry, Shandong University, Jinan 250100, China. E-mail: hgliu@sdu.edu.cn*

[b] *School of Physics and Electronics, Shandong Normal University, Jinan 250014, China. E-mail: minliyil@163.com*

[c] *Anastro Laboratory, Department of Chemistry, Changwon National University, Changwon 641-773, Korea*

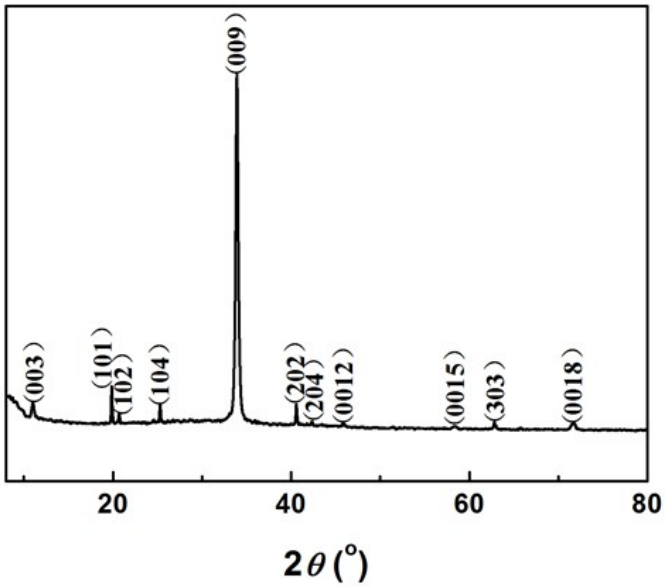

Fig. S1 XRD pattern of the nanoplates formed by adjusting the pH of the aqueous solution of lead acetate by NaOH solution.

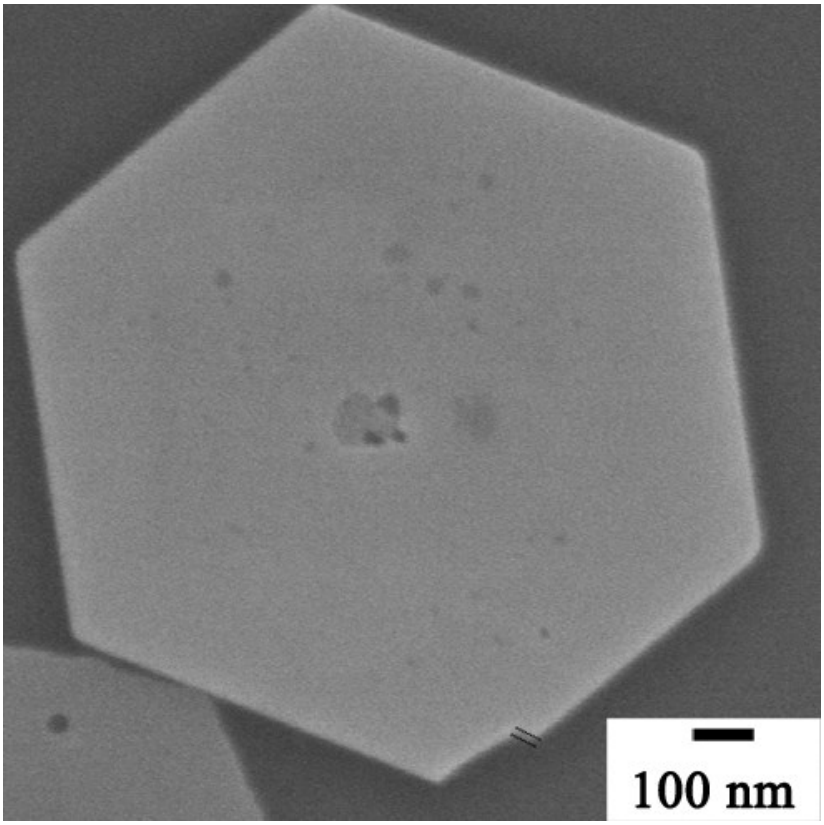

Fig. S2. SEM image of the nanoplates formed by mixing the aqueous solution of lead acetate with DMF.

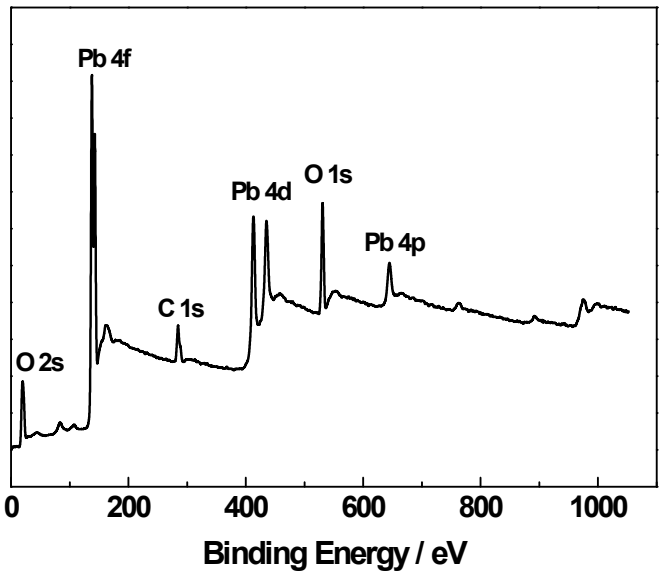

Fig. S3 XPS spectrum of the nanoplates formed by mixing the lead acetate aqueous solution with DMF.

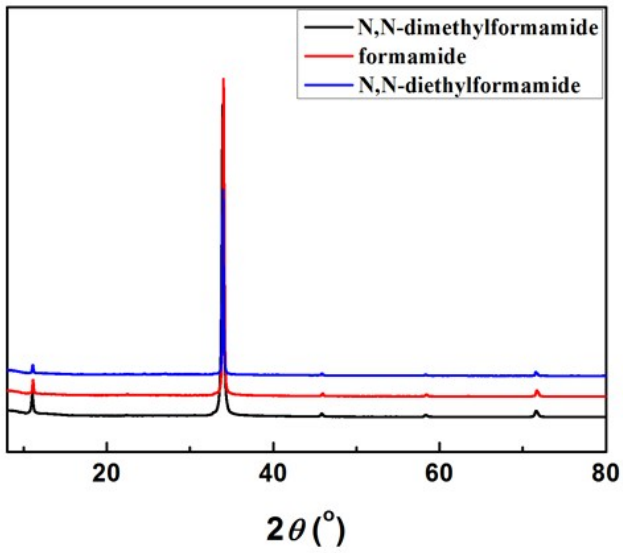

Fig. S4 XRD patterns of the nanoplates formed at ambient temperature by adding different organic base to the aqueous solution of lead acetate.

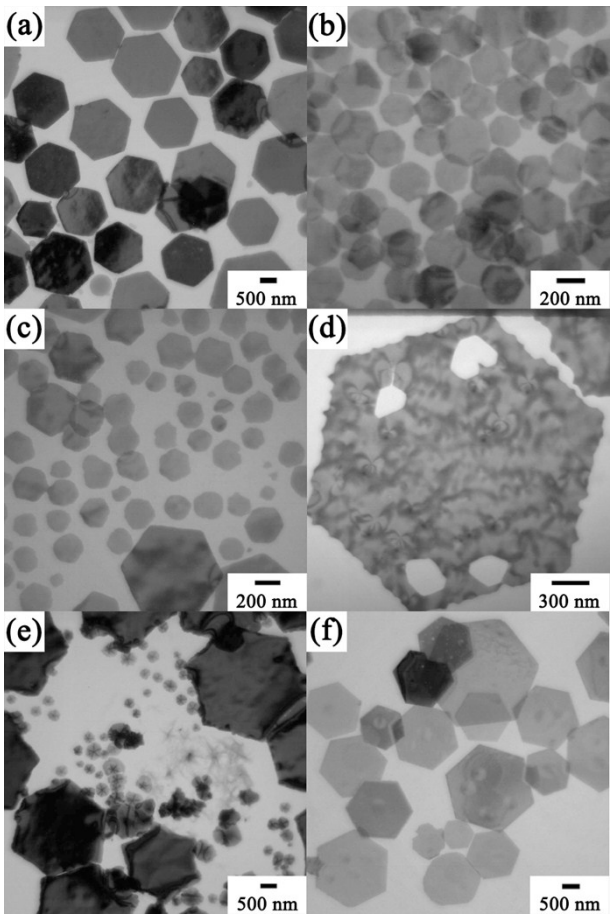

Fig. S5 TEM micrographs of the nanoplates formed at 40 (a-e) and 60°C (f). The volume ratio of the lead acetate aqueous solution and DMF is 1:1. The reaction times are 1 hour (a,f), 4 (b), 6 (c,d) and 8 hours (e), respectively.

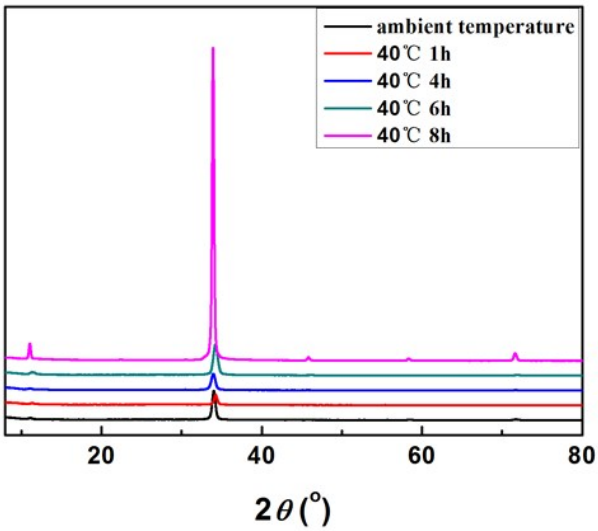

Fig. S6 XRD patterns of the nanoplates formed at ambient temperature and 40°C with different reaction time. The volume ratio of the lead acetate aqueous solution and DMF is 1:1.

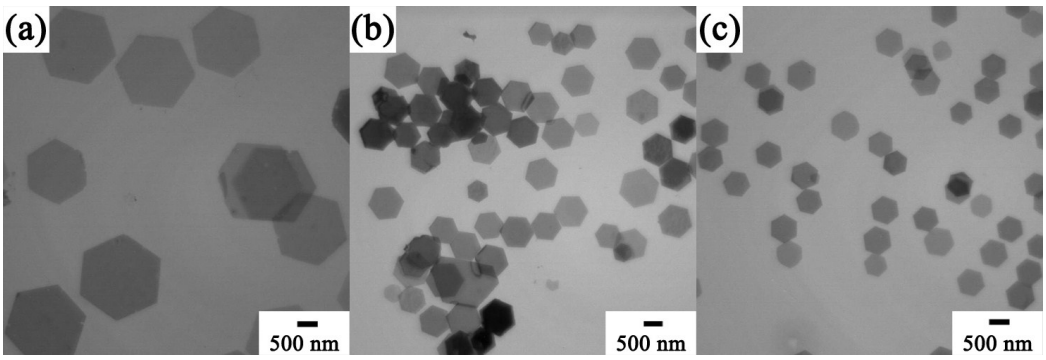

Fig. S7 TEM micrographs of the nanoplates formed at ambient temperature with different volume ratios of aqueous solution of lead acetate and DMF: (a), 8:2; (b), 4:6; (c), 3:7.

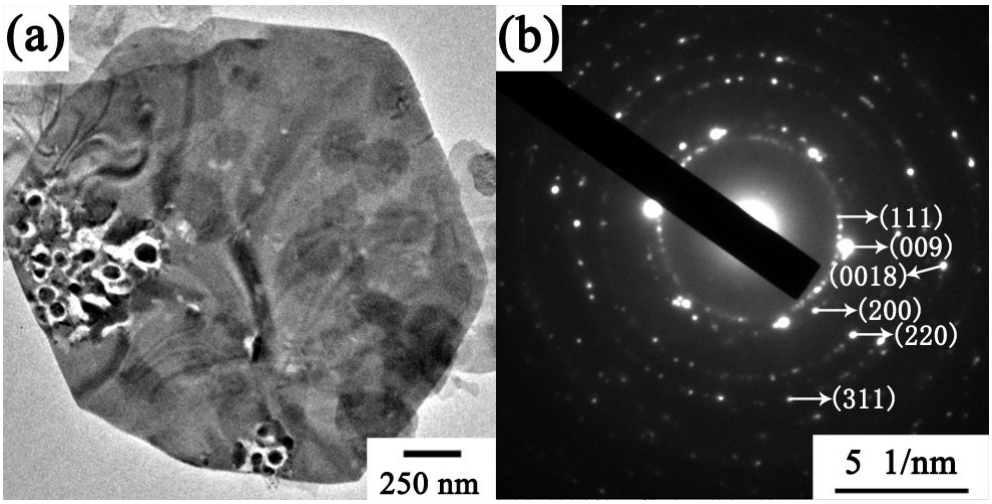

Fig. S8 TEM micrograph (a) and SAED pattern (b) of the nanoplates treated by 0.02 mol L^{-1} KBH_4 aqueous solution.

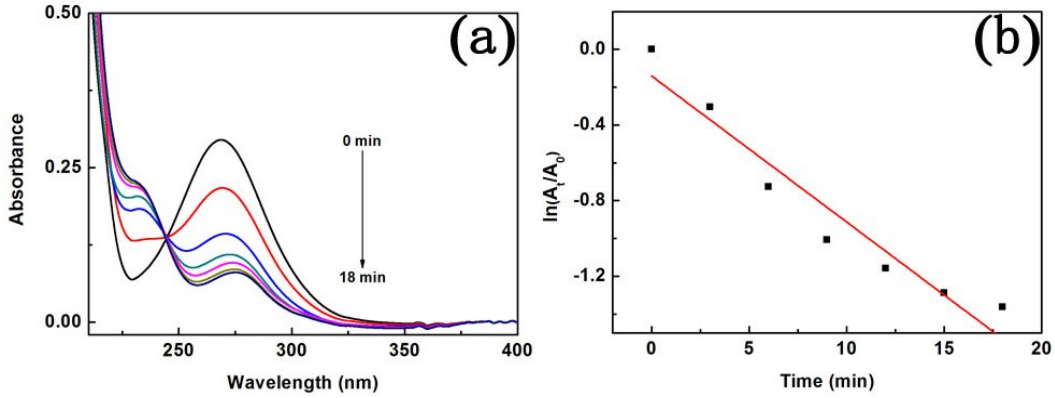

Fig. S9 Catalytic reduction of NB to aniline. Time-dependent absorption spectra (a) of the reaction solution in the presence of nanoplates deposited on a quartz slide and the corresponding plot of $\ln(A_t/A_0)$ against the reaction time (b)

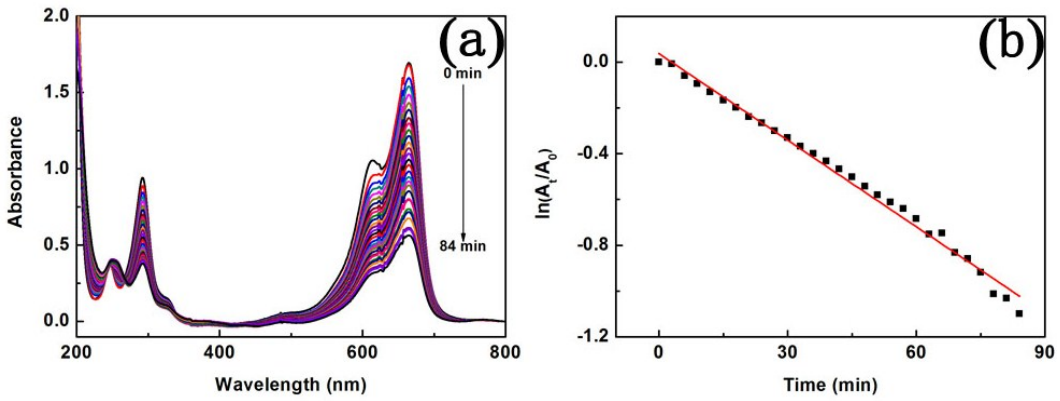

Fig. S10 Catalytic reduction of MB to leucomethylene blue (LMB). Time-dependent absorption spectra (a) of the reaction solution in the presence of nanoplates deposited on a quartz slide and the corresponding plot of $\ln(A_t/A_0)$ against the reaction time (b)

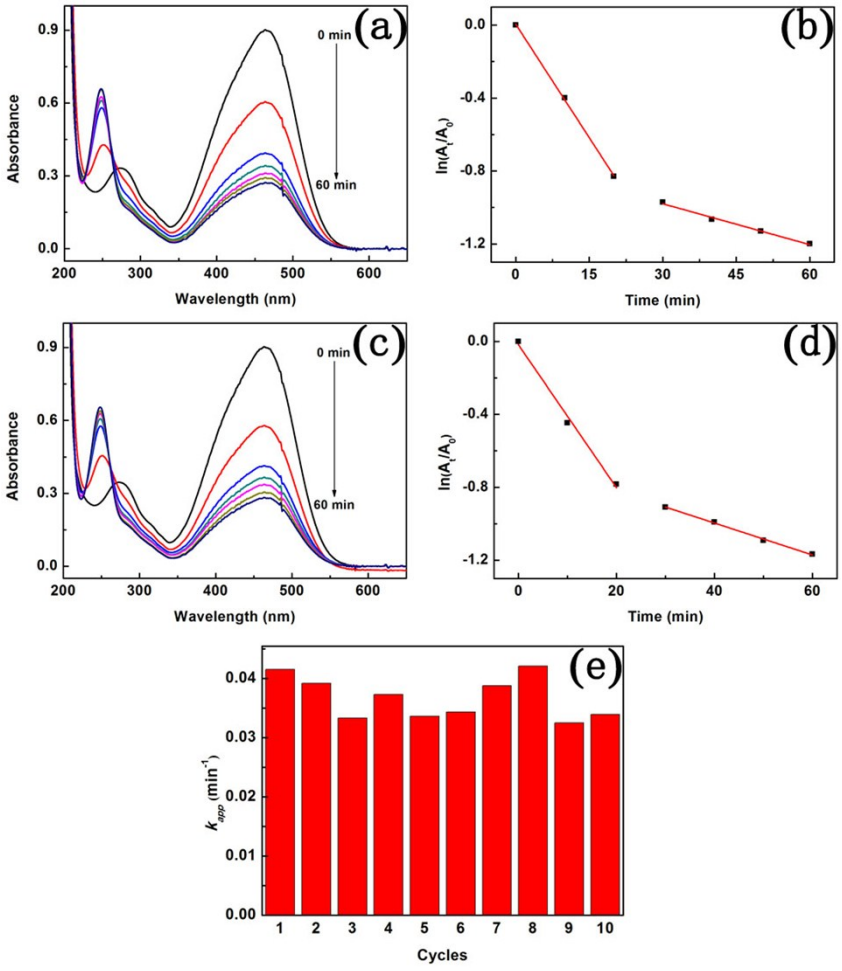

Fig. S11 Catalytic reduction of MO. Time-dependent absorption spectra (a, c) of the reaction solution in the presence of nanoplates deposited on a quartz slide, the corresponding plot of $\ln(A_t/A_0)$ against the reaction time (b, d) and the reaction rate constants in ten successive cycles (e). The reaction temperature is 308 K. The rate constants were obtained based on the fitting linear lines at the early stage of the reaction.

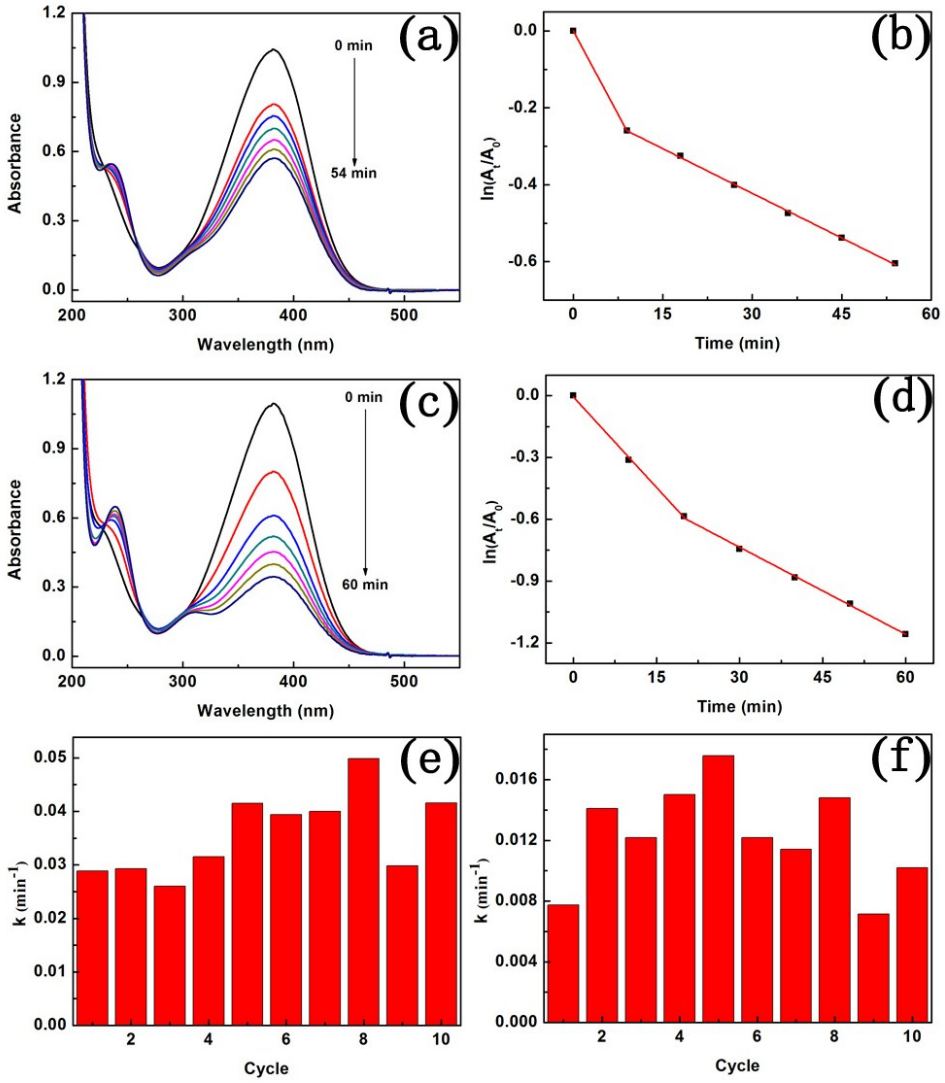

Fig. S12 Catalytic reduction of 4-NA to *p*-phenylenediamine. Time-dependent absorption spectra (a, c) of the reaction solution in the presence of nanoplates deposited on a quartz slide, the corresponding plot of $\ln(A_t/A_0)$ against the reaction time (b, d) and the reaction rate constants in ten successive cycles (e, f). The reaction temperature is 308 K. (a) and (c) correspond to the first and second cycles, respectively. The nanoplates were synthesized by tuning the pH of the aqueous solution of lead acetate with NaOH solution.

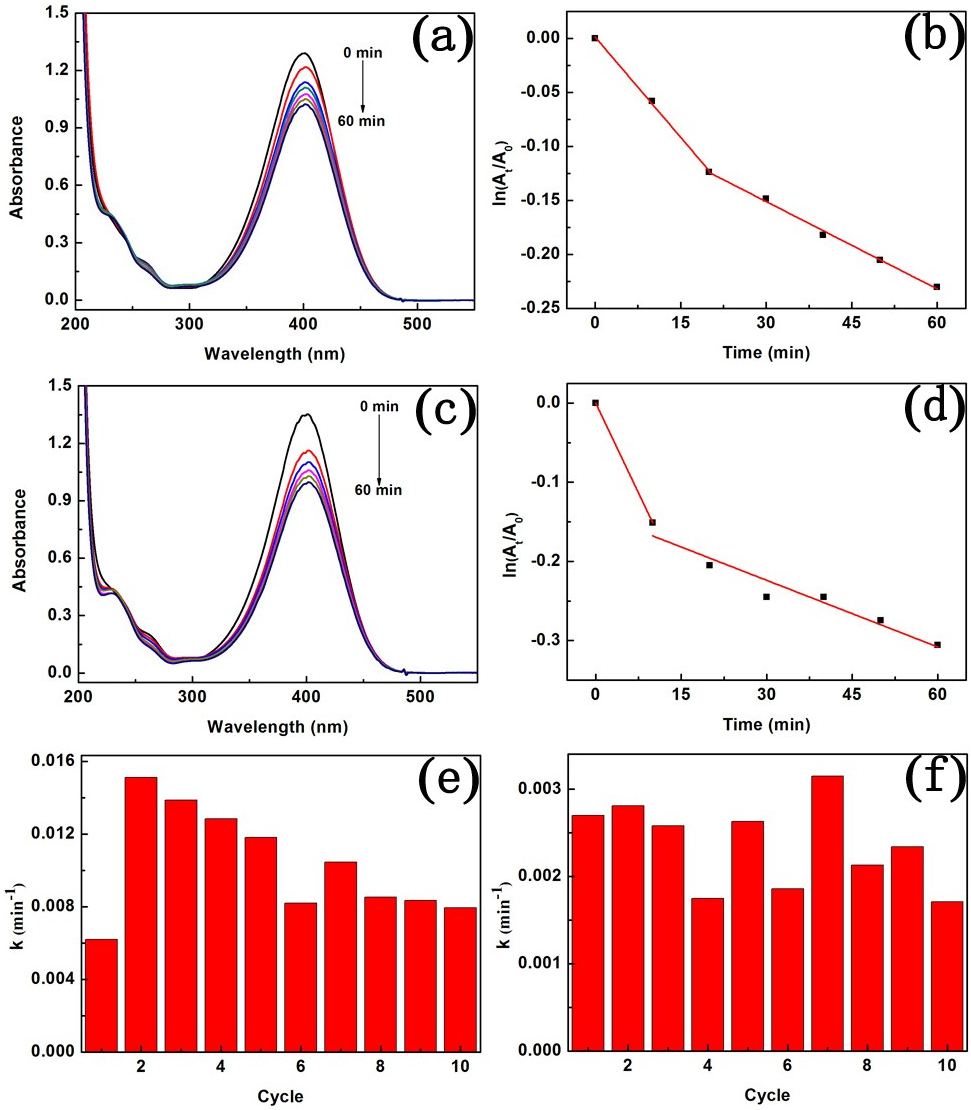

Fig. 13 Catalytic reduction of 4-NP to 4-AP. Time-dependent absorption spectra (a, c) of the reaction solution in the presence of nanoplates deposited on a quartz slide, the corresponding plot of $\ln(A_t/A_0)$ against the reaction time (b, d) and the reaction rate constants in ten successive cycles (e, f). The reaction temperature is 308 K. (a) and (c) correspond to the first and the second cycle, respectively. The rate constants were obtained based on the fitted linear lines at the early stage of the reaction. The nanoplates were synthesized by tuning the pH of the aqueous solution of lead acetate with NaOH solution.

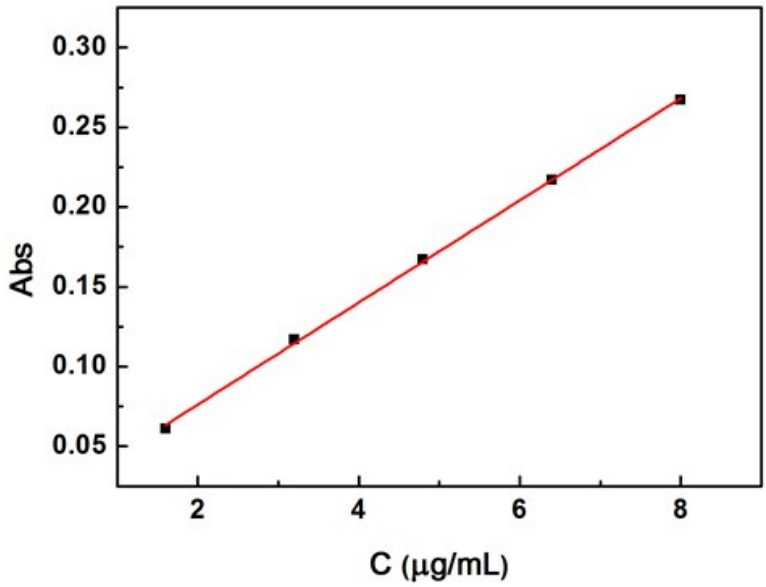

Fig. S14. Standard curve of the absorption intensities at 283.3 nm of Pb versus the concentrations of the standard Pb(II) aqueous solutions.

Fig. S14 shows the standard curve. The linear fitted equation is $A = 0.032c + 0.0122$, where A and c represent the absorption intensity and the concentration, respectively. Then the acidifying reaction solutions after the first cycle, the second cycle and the third cycle were tested, respectively. The A values were found to be 0.015, 0.007 and 0.010, corresponding to the Pb(II) concentrations of 0.09, -0.16 and -0.07 μg mL^{-1}, respectively based on the equation. These results indicate that a trace of Pb^{2+} ions exist in the acidifying solution after the first catalytic cycle, and almost no Pb^{2+} ion exists in the reaction solutions after the second and the third cycles.

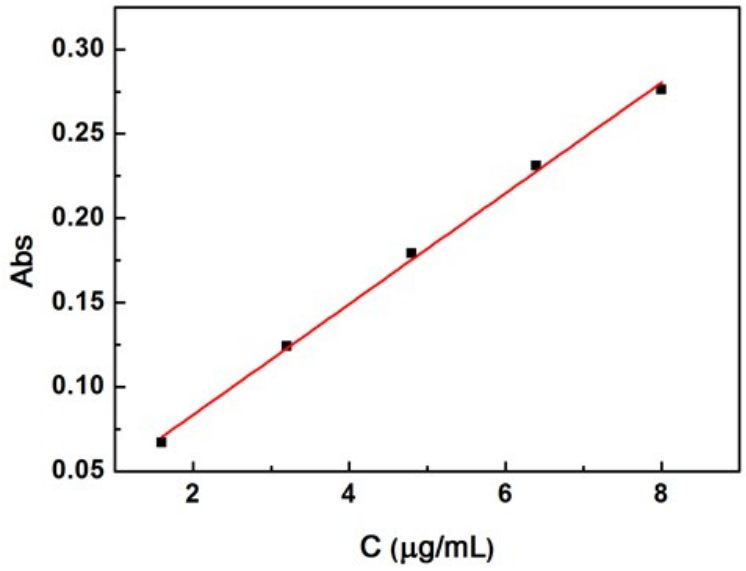

Fig. S15. Standard curve of the absorption intensities at 283.3 nm of Pb versus the concentrations of the standard Pb(II) aqueous solutions.

In order to clarify the existential state of the lead species in the first cycle reaction solution, this solution was examined directly using AAS without acidification. Fig S15 shows the standard curve. The fitted linear equation $A = 0.0328c + 0.0179$ was obtained. It was found that the absorption intensity at 283.3 nm was 0.009, which corresponded to the concentration of -0.27 μg mL^{-1}. This means no dissociative lead ions exist in the solution. Compared with the result of the acidifying solution, this indicated that the lead species exists in solid state. So it may be deduced that the lead species possible come from the detached nanoplate during the first reaction cycle. These nanoplates can be separated through centrifugation or filtration facilely. It should be noted that after the first cycle, the catalyst is very stable for the later cycles.